MATHEMATICAL MODELLING OF MALARIA DISEASE IN BUSIA COUNTY, KENYA

MOGAMBI NYASUGUTA LUCY

B. ED (SCIENCE)

156/CE/20480/2020

DEPARTMENT OF MATHEMATICS AND ACTUARIAL SCIENCE

A PROJECT SUBMITTED IN PARTIAL FULFILMENT OF THE REQUIREMENTS FOR THE AWARD OF THE DEGREE OF MASTER OF SCIENCE (APPLIED MATHEMATICS) IN THE SCHOOL OF PURE AND APPLIED SCIENCES OF KENYATTA UNIVERSITY

FEBRUARY, 2025

DECLARATION

This project is my original work and has not been submitted for any award of a degree in any University.

Name: Mogambi Nyasuguta Lucy

Signature: ..... Date: .....

Declaration by the Supervisor

This project has been submitted for examination with my approval at the University

Name: Dr. Mary Opondo

Signature: ..... Date: .....

Department of Mathematics and Actuarial Science, Kenyatta University

DEDICATION

I would like to dedicate this project to my sister Grace Kwamboka, my parents Christopher Keragia and Beatrice Mogambi and my siblings Cliff, Esther, Cynthia and Steve for their love and support.

ACKNOWLEDGEMENT

My special gratitude goes to my supervisor Dr. Mary Opondo for her guidance, encouragement and support she provided to me throughout this project. I also express my sincere appreciation to Kenyatta University for the chance awarded to me to pursue my MSc. Studies. Thanks to all my lecturers in the Mathematics Department at Kenyatta University for guiding me through this journey. I would also like to thank my beloved sister Grace Kwamboka for the financial support and motivation. Much appreciation to my parents and siblings for the emotional support they extended to me during my studies to this extent. Without forgetting, my special friend, Atunga Benson Kiage, for his continued and generous support he offered me throughout my academic journey. May God bless him abundantly. Above all, I thank God for all the blessings and sufficient grace that he has continuously shown me throughout my studies.

ABSRACT

Malaria remains a leading global health challenge, causing millions of deaths annually, primarily through the bite of infected female *Anopheles* mosquitoes. In Kenya, Busia County records the highest malaria prevalence at 37%, yet it has often been excluded from mathematical modeling studies. Traditional SEIR models commonly used in malaria research fail to capture the persistence of asymptomatic *Plasmodium* parasites in individuals who have recovered from the disease. This study introduces an enhanced SIRSp model that incorporates this asymptomatic subpopulation to better understand malaria dynamics in Busia County. The model assumes a constant infection rate influenced by both susceptible and infected individuals, and its mathematical analysis yields reproduction numbers for humans and mosquitoes. Stability analysis of the disease-free equilibrium point indicates the feasibility of eradicating malaria in Busia County under certain conditions. Numerical simulations demonstrate that higher infection rates significantly amplify the prevalence of malaria, whereas improving recovery rates reduces infections among humans and mosquitoes while marginally increasing the pool of susceptible individuals. These results provide valuable insights into the dynamics of malaria transmission and emphasize the importance of tailored interventions for effective disease management in endemic regions.

TABLE OF CONTENTS

LIST OF FIGURES

NOMENCLATURE

S_h Susceptible human subpopulation

I_h Infected human subpopulation

R_h Recovered human subpopulation

S_p Susceptible human subpopulation with *plasmodium* parasite

I_m Infectious mosquito subpopulation

S_m Susceptible mosquito subpopulation

N Total human population

α Proportion of human being infected when interacting with an infected mosquito

β Proportion of the susceptible mosquito being infectious when interacting with an infected human

M The mosquito population

Λ_h Rate of influx into the susceptible human subpopulation

Λ_m Rate of influx into the susceptible mosquito subpopulation

r Rate of recovery for an infected human being

γ Rate at which the recovered human being migrates to the susceptible human subpopulation

CHAPTER 1

INTRODUCTION

1.1 Background of the Study

Malaria is a historically persistent threat that has plagued tropical regions, significantly impacting health systems across Asia, the Americas, and Africa, which provide conducive environments for the disease's proliferation. This infectious disease is caused by protozoan parasites belonging to the genus *Plasmodium*, which invade and replicate within blood cells (Cai *et al*., 2017). Transmission to humans occurs primarily through the bite of an infected female *Anopheles* mosquito, with five *Plasmodium* species recognized as causative agents of malaria: *P. falciparum*, *P. vivax*, *P. ovale*, *P. malariae*, and *P. knowlesi* (Lashari et al., 2012). Among these species, the World Health Organization (WHO, 2019) identifies *P. falciparum* as the most virulent, with a high potential for mortality. This species is responsible for the majority of malaria-related morbidity and mortality in tropical and subtropical regions, as noted by Cai et al. (2017). Symptoms resulting from *P. falciparum* infection typically manifest within five hours post-bite and may include elevated body temperature, pain, fatigue, sweating, and shivering, as outlined by Ahmed *et al*. (2022). Malaria control has been hindered by the limited availability of effective antimalarial drugs and insufficient efforts towards the development of a robust vaccine, particularly in light of the evolving resistance observed in the *Plasmodium* parasites (Lashari et al., 2012).

According to the World Malaria Report by WHO (2021), there were 241 million malaria cases in 2020, an increase from 227 million in 2019. The estimated number of deaths in 2020 was 627,000, representing a rise of 69,000 from the previous year. The report highlights that 95% of malaria cases and 96% of deaths occurred in Sub-Saharan Africa, with children under five years of age accounting for 80% of the fatalities (WHO, 2021). The severity of malaria infection is closely linked to the immune response of the individual. Partial immunity develops over time

through repeated exposure to the parasite but tends to wane if reinfection does not occur. Importantly, infection with the malaria parasite does not always result in clinical disease. Many individuals in malaria-endemic regions remain asymptomatic, harboring significant parasite loads without exhibiting overt signs or symptoms. Furthermore, the epidemiology and transmission intensity of malaria vary across regions, influenced by local weather conditions and environmental factors. The World Health Organization (2019) has developed strategies to control and eliminate malaria transmission. Mathematical modeling has been instrumental in informing decision-making processes for designing effective intervention plans. However, relying on a single intervention is often insufficient to curb malaria spread in specific populations. For instance, in regions where *P. vivax* predominates, measures such as insecticide-treated nets (ITNs) and indoor residual spraying (IRS) may be less effective because mosquitoes typically bite early in the evening, take blood meals, and rest outdoors (WHO, 2019).

The health sector in Kenya has placed significant efforts in combatting the outbreak of malaria in Kenya and with the aim of reducing death from malaria by 75 per cent (Elnour et al., 2023). However, according to Bashir et al. (2019), majority of the Busia County population is susceptible to malaria due to poverty and insufficient health facilities. Busia County accounts for the largest malaria cases in Kenya. Malaria spread is extremely flexible in Busia County due to the varying climatic conditions. Malaria exists in four epidemiological zoning in Kenya: seasonal malaria transmission, malaria-free zones malaria endemic locations and malaria epidemic prone areas (WHO, 2019). These encounters call for crucial expansion of real and ideal policies for averting and regulating the spread of malaria. To overcome malaria in Kenya is therefore tantamount to overcoming it in Busia County. This study develops an appropriate $SIRS_p$ model to identify the trend and patterns in the outbreak of Malaria in Busia County of Kenya.

1.2 Definition of terms

Susceptible population: Refers to a member of the population who are at the risk of becoming infected by Malaria.

Stable population: Refers to a population with an unchanging structure of age and a secure degree of natural surge.

Mathematical modelling: Refers to the process of developing a mathematical model for disease control.

Endemic population: Refers to the constant presence of prevalence disease in a population within a given geographical area.

Infection rate: Refers to the probability or risk of an infection in a population. It's a measure of the frequency of occurrences of the infection in a given population.

1.3 Problem Statement

Most of the mathematical modelling approach follow the SEIR model for human population and SEI model among the vector population whereby the rate of infection be subject to the progress of the mosquitoes which hang on time. However, the paradigm is no longer applicable to the malaria disease due to current medical studies indicating that persons who have recovered from the infection still have the plasmodium parasites in their body system but in a latent stage. The malaria can reoccur again once the immunity decreases without the individual being bitten by an infected mosquito. This indicates that the $SIRS_p$ model in human population will be more appropriate. In our study, we shall focus on the host-vector model with $SIRS_p$ in human population towards preventing the spread of Malaria disease in Busia County, Kenya.

1.4 Objectives of the Study

1.4.1 General objective

To describe the dynamics of the spread of malaria disease with $SIRS_p$ model in Busia County, Kenya.

1.4.2 Specific objectives

The objectives of the study will be:

i. To simulate numerically the model to illustrate the behaviour of the model.

ii. To analyse the stability of the disease-free equilibrium for the control of the spread of malaria disease in Busia County, Kenya.

iii. To calculate the basic reproduction number, R_o.

iv. To optimise the parameters and obtain the optimal values for the parameters.

1.5 Justification

The SIRSp mathematical model has become an essential tool in understanding disease transmission dynamics and in supporting decision-making processes for designing effective malaria control interventions. The host-vector model with $SIRS_p$ in human population is a cost-effective and simple tool for achieving the greatest possible success in malaria eradication since by using this model, we can better understand the dynamics of malaria transmission and allocate resources to combat the disease.

1.6 Significance of the Study

This study aims to support policymakers in the health sector by advancing malaria eradication efforts through the application of the SIRSp mathematical modeling approach. The objective is to enhance public health outcomes, strengthen resistance to malaria, increase awareness of malaria prevalence, and propose effective control strategies. The findings of this research will provide valuable insights for local planners, the Ministry of Health, the Department of National Development, as well as key initiatives such as the 2030 Agenda for Sustainable Development and Kenya's Big Four Agenda, all of which play a critical role in shaping national health policy.

1.7 Assumptions

1. The disease's rate of infection in humans is constant.
2. Infection depends on the growth of the vector population, which depends on time (t), the number of people who are vulnerable, and the number of people who are already infected.
3. The newborn to be in the susceptible (S) compartment.

4. Some of those who have recovered from the infection will still carry *plasmodium* parasite and hence, such individuals enter the compartment S_p.
5. All parameters and variables are assumed to be non-negative.

CHAPTER 2

LITERATURE REVIEW

2.1 Mathematical Modelling of Malaria

Mathematical models have been studied to explore the spread and control of diseases in recent time. For instance, Zafar *et al.* (2022) studied the spread of human papillomavirus using the fractional-order derivatives and Bada *et al.* (2021) considered the spread of H7N9 virus using mathematical model. Specifically, the spread of diseases in Kenya has been investigated with the aid of mathematical modelling. Kimulu *et al.* (2022) modelled the spread of HIV in Kenya among sex workers with emphases on the interactions between the truckers and the sex workers on certain route in Kenya. The outcome of the study showed a reduction in the incidence rate of HIV. Furthermore, Andima *et al.* (2022) investigated the control of diabetes within the inadequate resources in Kenya using mathematical modelling. Mathematical modelling was also used by Kimulu *et al.* (2024) explore the spread of COVID-19 in Kenya.

Specifically, mathematical modelling of mosquito-borne diseases, particularly malaria, has proven to be an effective tool in understanding the dynamics of malaria spread and in formulating appropriate control strategies (Banerjee & Sanyal, 2023). Traditionally based on the SIR (Susceptible, Infected, Recovered) model, malaria modelling has evolved to incorporate various factors such as the malaria parasite's life cycle (Lashari *et al.*, 2012), the latent infection period (Cai *et al.*, 2017), immunity factors, and the interaction between human and mosquito populations (Cai *et al.*, 2019). Recent advancements in these models also account for the heterogeneous nature of both human and mosquito populations (Heath *et al.*, 2022), variations in exposure rates (Tchoumi *et al.*, 2023), and human recovery dynamics (Wang *et al.*, 2024).

Mojeeb *et al.* (2017) extended the model to SEIR (Susceptible, Exposed, Infected, Recovered) model to focus on the eradication of mosquito populations and the control of malaria outbreaks. Olaniyi *et al.* (2020) proposed a classification model that demonstrated the non-linear progression of malaria transmission, a finding that aligns with Mandal *et al.* (2011), who

developed a system to understand malaria disease propagation under various conditions. In a more specialized approach, Bakary et al. (2018) examined the impact of frequent mosquito bites and blood transfusions on malaria transmission dynamics. Additionally, Rafia et al. (2018) explored the effects of immunization on malaria transmission and disease severity, a topic also revisited by Mandal (2011), who used a model to evaluate the cyclical impacts of malaria epidemics, factoring in seasonal variations in mosquito bites and the fluctuating severity of outbreaks.

Recent work by Chen *et al*. (2024) introduces a hybrid model combining machine learning techniques with traditional epidemiological models, aiming to predict malaria outbreaks with greater accuracy by integrating environmental factors, such as temperature and rainfall, that influence mosquito breeding patterns. This research could provide valuable insights into the role of climate change in altering malaria transmission dynamics. Another recent study by Ale *et al*. (2024) explores the application of agent-based modelling in malaria, simulating interactions between individuals and mosquitoes at the local level to assess control interventions such as indoor spraying and insecticide-treated nets.

2.2 Global Approaches to Malaria Control Modelling

Mathematical models of disease infection often struggle to accurately account for multiple population classes, which is a significant limitation in modelling malaria dynamics. For malaria-infected populations, the SEIR (Susceptible, Exposed, Infected, Recovered) model has been widely employed to guide treatment strategies and control interventions (Mandal et al., 2011). These models aim to eradicate malaria by simulating interactions between humans and mosquitoes, incorporating factors such as infection latency and treatment strategies. Even under adverse conditions, such models predict that intervention efforts will significantly reduce mortality and morbidity compared to scenarios with no control measures (WHO, 2019).

One key challenge arises from the evolution of drug resistance. Resistance develops when spontaneous mutants with reduced drug sensitivity gain a survival advantage due to widespread

anti-malarial drug use. Mackinnon (2005) emphasized the need for cautious use of new anti-malarial drugs to reduce the selective pressure on parasites. Mandal et al. (2011) further argued that population-level interventions, such as widespread distribution of insecticide-treated bed nets (ITNs) or vaccines, may be more effective than individual-level approaches in preventing the emergence of drug resistance.

Recent trends include the use of dual-population models like SEIR-SEI, which account for human and mosquito dynamics in malaria control strategies. For example, Rwanda successfully utilized this framework to develop policies that significantly reduced infection rates (Osman & Adu, 2017; Cai et al., 2019). WHO (2019) has also highlighted that the eradication of diseases such as smallpox provides a blueprint for achieving malaria elimination targets, albeit with substantial challenges in adapting such strategies to malaria's unique dynamics.

Abongo (2016) applied conventional SEIR human models and SEI mosquito vector models in Kenya to evaluate the impact of various interventions. However, gaps remain, particularly in addressing vulnerable groups such as pregnant women, who are often excluded from control strategies despite being among the most at-risk populations. Recent studies by Carrasco-Escobar *et al*. (2021) propose incorporating socioeconomic factors and healthcare accessibility into malaria models to better capture the diverse challenges faced by vulnerable populations. Emerging research also focuses on integrating machine learning with traditional models to simulate the complex interactions between human and mosquito populations. A study by Ogbaga (2023) highlights the potential of AI-driven approaches to optimize resource allocation for interventions.

2.3 Challenges in Modelling Multiple Population Classes

The existence of several classes of population is a factor that the majority of mathematical models for disease infection cases twitch from. A population of people with malaria plague is anticipated to follow the SEIR model, which is intended for the treatment of malaria (Mandal *et al*., 2011). The goal of mathematical models of malaria sickness, which are industrialized from a variety of angles and include the interaction between humans and mosquitoes in the model of

malaria, is to eradicate the disease. Even in the worst-case scenario, it is expected that efforts to eradicate the disease will result in fewer deaths and illnesses overall than would occur if no action were taken (WHO, 2019). Consequently, anti-malarial drug fight occurs when impulsively arising mutants with abridged drug vulnerability are provided with advantage to survive by the use of the anti-malarial. The frugal use of new anti-malarial drugs has been suggested to diminish the discerning pressure of parasite (Mackinnon, 2005). Alternatively, Mandal *et al*. (2011) argue that population, rather than individual-level interventions like many first-line therapies, such as the distribution of a real vaccine or insecticide-treated bed nets (ITNs), could prevent the outbreak of drug resistance.

The SEIR-SEI mathematical model guided Rwanda's malaria control efforts, providing guidance to policymakers as they developed a plan to lower infection rates and rein in the disease (Osman & Adu, 2017; Cai *et al*., 2019). Furthermore, WHO (2019) notes that abolition of any disease is a determined aimed to achieve for smallpox and sanctioned diseasemarks for extermination.

Abongo (2016) used the conventional Susceptible-Exposed-Infectious-Recovered (SEIR) human models and the Susceptible-Exposed-Infectious (SEI) vector mosquito models in Kenyan malaria models for assessing the influence of interferences in perfect controls. Also, WHO (2019) endorsed defensive treatment for the greatest at-risk malaria group such as expectant women have not been included in the study in control theory options in Kenya.

2.4 The Need for Optimal Control Models in Kenya

Despite significant advancements in malaria control, there remains a critical gap in the development and application of optimal control models tailored to the unique transmission dynamics in Busia County, Kenya. Current efforts are hindered by the country's diverse transmission zones, which complicate the implementation of uniform strategies (DOMC, 2010). Notably, there is no existing optimal control model that integrates four control variables while addressing the specific challenges of malaria invasion research, such as those related to intermittent preventive treatment during pregnancy (IPTp) (WHO, 2019).

This gap highlights the pressing need for mathematical models that incorporate host-vector dynamics, such as the SIRSp model, specifically adapted to the human population in Busia County. Such models could provide actionable insights into reducing malaria transmission and inform the design of regionally appropriate interventions. Moreover, raising awareness about the potential of these scientific tools among policymakers and public health stakeholders is crucial for mitigating the devastating impact of malaria in this high-risk region. By addressing this research gap, future studies can contribute to the development of evidence-based strategies for malaria control, thereby enhancing the effectiveness of existing interventions and supporting Kenya's broader malaria elimination goals.

CHAPTER 3

RESEARCH METHODOLOGY

3.1 Model Development

Two populations are in play here; the human population in Busia County and the mosquito population in Busia County, where each of the populations has the tendency to influence the presence of malaria in the ecosystem. The interaction and migrations between the subpopulations are shown in the model description of figure (3.1). The directional arrows indicate migration from a subpopulation to another, the dashed non-directional lines indicate interactions without migration (clearly, human population cannot migrate into the mosquito subpopulation and vice versa). The human subpopulations are represented in the blue boxes while the mosquito subpopulations are represented in the red boxe

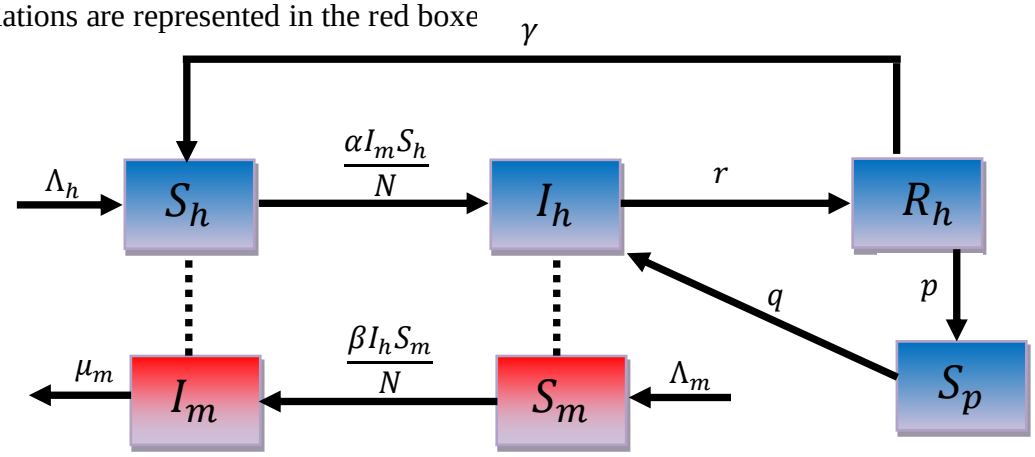

Figure 3.1: Model Description

The human population is divided into four subpopulations; the susceptible human subpopulation S_h, the infected human subpopulation I_h , the recovered human subpopulation R_h and the susceptible with plasmodium parasite human subpopulation S_p. The mosquito is subdivided into the infectious mosquito subpopulation I_m and the susceptible mosquito subpopulation S_m. The susceptible human subpopulation gets infected when there is an interaction with an infected mosquito with the force of infection

$$\frac{\alpha I_m S_h}{N}$$

where N is the total human population, α is the proportion of interaction that led to infection. The susceptible mosquitoes become infectious by interacting with the malaria-infected human subpopulation with the rate of infection

$$\frac{\beta I_h S_m}{M},$$

where β is the proportion of interaction that led to infection and M is the population of mosquitoes. The rate of influx into the susceptible human subpopulation and susceptible mosquito subpopulation are Λ_h and Λ_m respectively. An infected human recovers from malaria at the rate r and it is assumed that a recovered human migrates to the susceptible human subpopulation at the rate γ. By writing out the rate of change of each subpopulation, the equations governing the malaria trend in the population is the system of equations (3.1.1) – (3.1.6).

$$\frac{dS_h}{dt} = \Lambda_h + \gamma R_h - \frac{\alpha I_m S_h}{N} \tag{3.1.1}$$

$$\frac{dI_h}{dt} = \frac{\alpha I_m S_h}{N} - rI_h + qS_p \tag{3.1.2}$$

$$\frac{dS_p}{dt} = pR_h - qS_p \tag{3.1.3}$$

$$\frac{dR_h}{dt} = rI_h - \gamma R_h - pR_h \tag{3.1.4}$$

$$\frac{dS_m}{dt} = \Lambda_m - \frac{\beta I_h S_m}{M} \tag{3.1.5}$$

$$\frac{dI_m}{dt} = \frac{\beta I_h S_m}{M} - \mu_m I_m \tag{3.1.6}$$

with the following initial conditions (3.1.7)

$$\begin{cases} S_h(0) = S_h^0 > 0, \\ I_h(0) = I_h^0 \geq 0, \\ R_h(0) = R^0 \geq 0, \\ S_p(0) = S_{p,h}(0) \geq 0, \\ S_m(0) = S_m^0 > 0, \\ I_m(0) = I_m^0 \geq 0. \end{cases} \tag{3.1.7}$$

The parameters are also restricted to the conditions in (3.1.8) as

$$0 < \Lambda_h, \Lambda_m, \gamma, \alpha, \beta, r, \mu_m, p, q < 1, \tag{3.1.8}$$

3.2 Reproduction Numbers

The human and mosquito populations remain susceptible until an infectious mosquito gets into the population and infection happens as a result of interaction between the infectious mosquito and susceptible humans or interaction between a susceptible mosquito and an infected human. The rate at which susceptible human population gets infected by the introduction of one infectious mosquito into the population is the reproduction number for mosquito while the rate at which susceptible mosquito population becomes infectious by the introduction of one infected human into the population is the reproduction number for human (Abimbade *et al*., 2022; Aldila, 2022). These reproduction numbers are calculated by investigating the rate of change of the infectious class according to equations (3.1.2) and (3.1.6). Considering when a single infectious mosquito is brought into the susceptible human subpopulation, indicating that $I_m = 1$ and $S_h = N$, therefore equation (3.1.2) becomes

$$\frac{dI_h}{dt} = \alpha - r = r\left(\frac{\alpha}{r} - 1\right).$$

By setting $R_{h,0} = \frac{\alpha}{r}$ as the reproduction number for the malaria infection in the human population, then

$$\frac{dI_h}{dt} = r\left(R_{h,0} - 1\right). \tag{3.2.1}$$

Equation (3.2.1) shows that the infection in the human population dies out if $R_{h,0} < 1$ but remains endemic if $R_{h,0} > 1$.

Similarly, when one malaria-infected human is brought into the population, where no mosquito is infectious, indicating that $I_h = 1$ and $S_m = M$, then equation (3.1.6) becomes

$$\frac{dI_m}{dt} = \beta - \mu_m = \mu_m \left(\frac{\beta}{\mu_m} - 1\right). \tag{3.2.2}$$

By setting $R_{m,0} = \frac{\beta}{\mu_m}$ in (3.2.2) as the reproduction numbers for the mosquitoes to get infectious, then

$$\frac{dI_m}{dt} = \mu_m\left(R_{m,0} - 1\right). \tag{3.2.3}$$

Hence, if $R_{h,0} < 1$, then the mosquitoes do not become infectious.

3.3 Numerical Solution

The adaptive step-size method is used to solve the model equations (3.1.1) – (3.1.6). The method involves the adjustment of the step-size during numerical integration by taking note of the behaviour of the solution during each iteration. The Runge-Kutta-Fehlberg (RKF45) method is adopted in this study (see Amoo *et al*. (2022), Oke (2017) and Montijano *et al*. (2024) for details). RKF45 smoothly combines Runge-Kutta of order 4 with order 5 by reducing the local truncation error. The problem under consideration can be written as

$$\frac{d}{dt}\boldsymbol{X} = \boldsymbol{F}(\boldsymbol{X}), \quad \boldsymbol{X}_0 = \boldsymbol{X}(t_0), \tag{3.3.1}$$

where $\boldsymbol{X} = (S_h, I_h, R_h, S_m, I_m)^T$. The RKF45 algorithm for numerically solving the problem (3.3.1) under consideration is as follows;

STEP 1: Initialise the step-size h_0, time t_0 and the value of the variables $\boldsymbol{X}_0$.

STEP 2: Solve the problem with both Runge-Kutta of order 4 and of order 5. The RKF45 scheme is as follows;

$$\boldsymbol{K}_1 = h\boldsymbol{F}(t_n, \boldsymbol{X}_n),$$

$$\boldsymbol{K}_2 = h\boldsymbol{F}\left(t_n + \frac{h}{4}, \boldsymbol{X}_n + \frac{1}{4}\boldsymbol{K}_1\right),$$

$$\boldsymbol{K}_3 = h\boldsymbol{F}\left(t_n + \frac{3h}{8}, \boldsymbol{X}_n + \frac{3}{32}\boldsymbol{K}_1 + \frac{9}{32}\boldsymbol{K}_2\right),$$

$$\boldsymbol{K}_4 = h\boldsymbol{F}\left(t_n + \frac{12h}{13}, \boldsymbol{X}_n + \frac{1932}{2197}\boldsymbol{K}_1 - \frac{7200}{2197}\boldsymbol{K}_2 + \frac{7296}{2197}\boldsymbol{K}_3\right),$$

$$\boldsymbol{K}_5 = h\boldsymbol{F}\left(t_n + h, \boldsymbol{X}_n + \frac{439}{216}\boldsymbol{K}_1 - 8\boldsymbol{K}_2 + \frac{3680}{513}\boldsymbol{K}_3 - \frac{845}{4104}\boldsymbol{K}_4\right),$$

$$\boldsymbol{K}_4 = h\boldsymbol{F}\left(t_n + \frac{h}{2}, \boldsymbol{X}_n - \frac{8}{27}\boldsymbol{K}_1 + 2\boldsymbol{K}_2 - \frac{3544}{2565}\boldsymbol{K}_3 + \frac{1859}{4104}\boldsymbol{K}_4 - \frac{11}{40}\boldsymbol{K}_5\right),$$

$$\boldsymbol{X}_{n+1}^{\mathbf{5}} = \boldsymbol{X}_n^{\mathbf{5}} + \frac{25}{216}\boldsymbol{K}_1 + \frac{1408}{2565}\boldsymbol{K}_3 + \frac{2197}{4104}\boldsymbol{K}_4 - \frac{1}{5}\boldsymbol{K}_5.$$

$$\boldsymbol{X}_{n+1}^{\mathbf{5}(*)} = \boldsymbol{X}_n^{\mathbf{5}} + \frac{16}{135}\boldsymbol{K}_1 + \frac{6656}{12825}\boldsymbol{K}_3 + \frac{28561}{56430}\boldsymbol{K}_4 - \frac{9}{50}\boldsymbol{K}_5 + \frac{2}{55}\boldsymbol{K}_{\mathbf{6}}.$$

STEP 3: Estimate the local error

$$E = \left|\boldsymbol{X}_{n+1}^{\mathbf{5}} - \boldsymbol{X}_{n+1}^{\mathbf{5}(*)}\right| \tag{3.3.2}$$

STEP 4: If $E <$ tolerance, then X_{n+1}^5 is accepted as the solution at that time step and step-size for the next iteration is adjusted as

$$h_{n+1} = h_n\left(\frac{\text{tolerance}}{E}\right)^{\frac{1}{5}}. \tag{3.3.3}$$

Else, reject the solution and reduce h_n and repeat STEP 2

STEP 5: Repeat Steps 1 – 4 until the final time is reached.

3.4 Equilibrium points and stability

Consider the critical point of the equations (3.1.1) – (3.1.6) where all equations are equated to zero so that

$$\Lambda_h + \gamma R_h - \frac{\alpha I_m S_h}{N} = 0 \tag{3.3.4}$$

$$\frac{\alpha I_m S_h}{N} - rI_h + qS_p = 0 \tag{3.3.5}$$

$$pR_h - qS_p = 0 \tag{3.3.6}$$

$$rI_h - \gamma R_h - pR_h = 0 \tag{3.3.7}$$

$$\Lambda_m - \frac{\beta I_h S_m}{M} = 0 \tag{3.3.8}$$

$$\frac{\beta I_h S_m}{M} - \mu_m I_m = 0 \tag{3.3.9}$$

3.4.1 Disease-free equilibrium

Firstly, the disease-free equilibrium point can be found by setting $I_h = 0$ in all equations. To

start with equation (3.3.8), we have

$$\Lambda_m - \frac{\beta \times 0 \times S_m}{M} = 0 \quad \Rightarrow \quad \Lambda_m = 0.$$

Next consider equation (3.3.7)

$$(r \times 0) - (\gamma + p)R_h = 0 \ \Rightarrow \ -(\gamma + p)R_h = 0 \ \Rightarrow R_h = 0.$$

Set $R_h = 0$ and $I_h = 0$ in equation (3.3.6) and (3.3.9) and we have

$$(p \times 0) - qS_p = 0 \ \Rightarrow \ -qS_p = 0 \ \Rightarrow \ S_p = 0.$$

$$\frac{\beta \times 0 \times S_m}{M} - \mu_m I_m = 0 \ \Rightarrow \ -\mu_m I_m = 0 \ \Rightarrow \ I_m = 0.$$

Equation (3.3.5) is automatically satisfied since $I_m = I_h = S_p = 0$. Substituting all the other variables into equation (3.3.4) gives

$$\Lambda_h + (\gamma \times 0) - \frac{\alpha \times 0 \times S_h}{N} = 0 \ \Rightarrow \ \Lambda_h = 0.$$

Hence, the disease-free equilibrium is therefore

$$\left(S_h^{DFE}, I_h^{DFE}, S_p^{DFE}, {R_h}^{DFE}, S_m^{DFE}, I_m^{DFE}\right) = (\xi, 0,0,0, \sigma, 0) \qquad (3.4.1.1)$$

where $\Lambda_m = \Lambda_h = 0$ and ξ, σ are arbitrary values.

3.4.2 Other equilibrium points

However, other equilibrium points exist. We start by making R_h the subject from equation (3.3.7), we have

$$R_h = \frac{r}{\gamma + p} I_h. \qquad (3.4.1.2)$$

From (3.3.8) and (3.3.9), we have

$$S_m = \frac{M\Lambda_m}{\beta I_h} \qquad (3.4.2.1)$$

$$S_m = \frac{M\mu_m I_m}{\beta I_h}, \qquad (3.4.2.2)$$

respectively. Hence, equating (3.4.2.1) and (3.4.2.2) implies

$$\frac{M\Lambda_m}{\beta I_h} = \frac{M\mu_m I_m}{\beta I_h} \quad \Rightarrow \quad I_m = \frac{\Lambda_m}{\mu_m}. \qquad (3.4.2.3)$$

It is easy to see from equation (3.3.6) that

$$S_p = \frac{p}{q} R_h = \frac{pr}{q(\gamma + p)} I_h. \tag{3.4.2.4}$$

Looking at equation (3.3.5),

$$S_h = \frac{N(rI_h - qS_p)}{\alpha I_m}$$

$$= \frac{N\mu_m}{\alpha \Lambda_m}(rI_h - qS_p),$$

$$= \frac{N\mu_m}{\alpha \Lambda_m}\left(rI_h - \frac{pr}{(\gamma + p)} I_h\right),$$

$$= \frac{N\mu_m r}{\alpha \Lambda_m}\left(1 - \frac{p}{(\gamma + p)}\right) I_h.$$

Hence,

$$S_h = \frac{N\mu_m r\gamma}{\alpha \Lambda_m (\gamma + p)} I_h. \tag{3.4.2.5}$$

Finally consider (3.3.4), we have

$$\Lambda_h + \gamma\left(\frac{r}{\gamma} I_h\right) - \frac{\alpha}{N}\left(\frac{\Lambda_m}{\mu_m}\right)\left(\frac{rN\mu_m\gamma}{\alpha\Lambda_m(\gamma + p)} I_h\right) = 0$$

$$\Lambda_h + rI_h - \frac{r\gamma}{(\gamma + p)} I_h = 0.$$

$$\Lambda_h + \left(1 - \frac{\gamma}{(\gamma + p)}\right) rI_h = 0.$$

$$\Lambda_h + \frac{pr}{(\gamma + p)} I_h = 0.$$

and therefore

$$I_h = -\frac{(\gamma + p)\Lambda_h}{pr}. \tag{3.4.2.6}$$

Since all parameters are greater than zero, then $I_h < 0$. This is not physically possible and hence we say there are no other equilibrium points other than the disease-free equilibrium point.

3.4.3 Stability

The Jacobian of the system (3.1.1) – (3.1.6) is obtained by assembling the derivatives of the right-hand side of the equations with respect to all the variables $S_h,\ I_h,\ S_p,\ R_h,\ S_m$ and I_m. The resulting matrix called the Jacobian is as follows;

$$\begin{pmatrix} -\frac{\alpha I_m}{N} & 0 & 0 & \gamma & 0 & -\frac{\alpha S_h}{N} \\ \frac{\alpha I_m}{N} & -r & q & 0 & 0 & \frac{\alpha S_h}{N} \\ 0 & 0 & -q & p & 0 & 0 \\ 0 & r & 0 & -\gamma - p & 0 & 0 \\ 0 & -\frac{\beta S_m}{M} & 0 & 0 & -\frac{\beta I_h}{M} & 0 \\ 0 & \frac{\beta S_m}{M} & 0 & 0 & \frac{\beta I_h}{M} & -\mu_m \end{pmatrix}.$$

The eigenvalues of the system can be found by solving the characteristic equation

$$\begin{vmatrix} -\frac{\alpha I_m}{N} - \lambda & 0 & 0 & \gamma & 0 & -\frac{\alpha S_h}{N} \\ \frac{\alpha I_m}{N} & -r - \lambda & q & 0 & 0 & \frac{\alpha S_h}{N} \\ 0 & 0 & -q - \lambda & 0 & 0 & 0 \\ 0 & r & 0 & -\gamma - p - \lambda & 0 & 0 \\ 0 & -\frac{\beta S_m}{M} & 0 & 0 & -\frac{\beta I_h}{M} - \lambda & 0 \\ 0 & \frac{\beta S_m}{M} & 0 & 0 & \frac{\beta I_h}{M} & -\mu_m - \lambda \end{vmatrix} = 0.$$

Evaluating the characteristic equation at the DFE by substituting

$$\left(S_h^{DFE}, I_h^{DFE}, S_p^{DFE}, {R_h}^{DFE}, S_m^{DFE}, I_m^{DFE}\right) = (\xi, 0,0,0, \sigma, 0),$$

gives;

$$\begin{vmatrix} -\lambda & 0 & 0 & \gamma & 0 & -\frac{\alpha \xi}{N} \\ 0 & -r - \lambda & q & 0 & 0 & \frac{\alpha \xi}{N} \\ 0 & 0 & -q - \lambda & 0 & 0 & 0 \\ 0 & r & 0 & -\gamma - p - \lambda & 0 & 0 \\ 0 & -\frac{\beta \sigma}{M} & 0 & 0 & -\lambda & 0 \\ 0 & \frac{\beta \sigma}{M} & 0 & 0 & 0 & -\mu_m - \lambda \end{vmatrix} = 0.$$

Evaluating the determinant along the first column gives

$$-\lambda\begin{vmatrix} -r-\lambda & q & 0 & 0 & \frac{\alpha\xi}{N} \\ 0 & -q-\lambda & 0 & 0 & 0 \\ r & 0 & -\gamma-p-\lambda & 0 & 0 \\ -\frac{\beta\sigma}{M} & 0 & 0 & -\lambda & 0 \\ \frac{\beta\sigma}{M} & 0 & 0 & 0 & -\mu_m-\lambda \end{vmatrix} = 0.$$

Further evaluating the determinant along the third column gives

$$-\lambda(-\gamma-p-\lambda)\begin{vmatrix} -r-\lambda & q & 0 & \frac{\alpha\xi}{N} \\ 0 & -q-\lambda & 0 & 0 \\ -\frac{\beta\sigma}{M} & 0 & -\lambda & 0 \\ \frac{\beta\sigma}{M} & 0 & 0 & -\mu_m-\lambda \end{vmatrix} = 0.$$

Even further evaluation of the determinant along the third column gives

$$\lambda^2(-\gamma-p-\lambda)\begin{vmatrix} -r-\lambda & q & \frac{\alpha\xi}{N} \\ 0 & -q-\lambda & 0 \\ \frac{\beta\sigma}{M} & 0 & -\mu_m-\lambda \end{vmatrix} = 0.$$

Finally, evaluate the determinant along the second row,

$$\lambda^2(-\gamma-p-\lambda)(-q-\lambda)\begin{vmatrix} -r-\lambda & \frac{\alpha\xi}{N} \\ \frac{\beta\sigma}{M} & -\mu_m-\lambda \end{vmatrix} = 0.$$

Which finally becomes

$$\lambda^2(-\gamma-p-\lambda)\left((\lambda+\mu_m)(r+\lambda)+\frac{\beta\alpha\sigma\xi}{MN}\right) = 0.$$

$$\Rightarrow \lambda = 0, \quad -\gamma-p \quad \text{and} \quad \lambda^2+(r+\mu_m)\lambda+r\mu_m+\frac{\beta\alpha\sigma\xi}{MN} = 0 \qquad (3.4.3.1)$$

Since $\alpha, \beta, M, N, \sigma, \xi, p, q > 0$, then the root of $\lambda^2+(r+\mu_m)\lambda+r\mu_m+\frac{\beta\alpha\sigma\xi}{MN} = 0$ are all negative. Therefore, the DFE is always stable.

3.5 Parameter optimisation

Estimation of the most appropriate values for the parameters is important in the modelling of malaria due to the nature of the disease. Malaria is a non-communicable disease that requires two separate immiscible populations; hence, the next step is to estimate values for the parameters. The variable that can be easily obtained is the number of infected Kenyans and as such we optimise the parameters using the infected human population. In this case, the observed number of infected human population over a period of time is recorded in the vector $\boldsymbol{x_0}(t_k)$ while the model equations (3.1.1) – (3.1.6) is solved over the same time interval and the numerical result for the infected human population is stored in the vector $\boldsymbol{x}(t_k, \Theta)$ where $\Theta = (\Lambda_h, \Lambda_m, \gamma, \alpha, \beta, r, \mu_m)$ is the parameter vector which are to be optimised. The objective function is now written as

$$\text{minimise} \quad \Theta = \sum_{k=1}^{N} |\boldsymbol{x}(t_k, \Theta) - \boldsymbol{x}_0(t_k)|^2. \tag{3.5.1}$$

The parameters, as stated in equation (3.1.8), are bounded in the interval $[0,1]$ and hence we set the bounds to the parameters as follows;

$$0 < \Lambda_h < 1$$

$$0 < \Lambda_m < 1,$$

$$0 < \gamma < 1,$$

$$0 < \alpha < 1,$$

$$0 < \beta < 1,$$

$$0 < r < 1,$$

$$0 < \mu_m < 1.$$

The Broyden-Fletcher-Goldfarb-Shanno (BFGS) method is used to minimise the objective function. BFGS is a quasi-Newton method that iteratively approximates the inverse Hessian matrix in the search for the optimal solution (Xue *et al*., 2022; Luo *et al*., 2022). The update rule is set by the equation

$$B_{k+1} = B_k + \frac{(\Delta x_k)(\Delta x_k)^T}{(\Delta x_k)^T(\Delta s_k)} - \frac{B_k s_k s_k^T B_k}{s_k^T B_k s_k}$$

where B_k is the inverse Hessian matrix approximation, Δx_k is the gradients change and Δs_k is the change in the search parameter values and the search direction is

$$d_k = -B_k \nabla f(x_k).$$

The "minimize" function in Python SciPy contains the BFGS method and as such is used in this study to find the optimal values for the optimal parameters. The optimal values of the parameters are kept fixed while solving the model equations (3.1.1) – (3.1.6) and varying one parameter at a time to investigate the behaviour of the population under various conditions.

CHAPTER 4

RESULTS AND DISCUSSION

4.1 Introduction

Malaria infection has been modelled as a system of first order nonlinear ordinary differential equations (3.1.1) – (3.1.6). In this chapter, the optimal values of the parameters are obtained and discussed, the model is simulated for the various parameters to estimate and the results are graphed and discussed.

4.2 Parameter Optimisation

The parameter optimization process involves comparing two datasets: real-world data and data generated from the mathematical model. Real-world malaria cases recorded between 2010 and 2021 were obtained from the Statista website[1] and summarized in Table 4.1. This dataset, derived from reliable WHO records, reflects the malaria burden in Busia County, Kenya, over a decade. The population values, expressed in units of ten thousand, highlight significant demographic changes during the study period.

Table 4.1:Malaira cases in Busia County, Kenya from 2010 to 2021 (Source: WHO, 2021)

Year	2010	2011	2012	2013	2014	2015	2016	2017	2018	2019	2020	2021
Population (in ten thousand)	0.90	1	1.45	2.37	2.85	2.04	3.06	3.60	3.32	5.02	3.66	3.83

The data from the numerical integration of the model is optimised in Python using the code in figure (4.1). As shown in figure (4.1), the model equations and the objective function are defined and the numerical solution is obtained by calling the `odeint` command. The numerical solution is stored in the `solution`. Optimisation of the parameters is done by comparing the numerical results with the real-world data in Table (4.1). The optimal parameter values are thus obtained as;

[1] https://www.statista.com/statistics/1240010/number-of-malaria-cases-in-kenya/#:~:text=In%202021%2C%20nearly%203.83%20million,health%20issues%20in%20the%20country.

$$\Lambda_h = 1, \gamma = 1, \alpha = 1, r = 0.39195362, \Lambda_m = 1, \beta = 1, \mu_m = 0.$$

The validity of the optimised parameters was assessed by plotting the infected human subpopulation generated by the model against real-world malaria case data, as shown in Figure 4.2. The results indicate strong agreement between the model predictions and the empirical data, particularly as time progresses. This alignment suggests that the chosen parameters effectively capture the dynamics of malaria transmission in Busia County.

```
# Function representing the system of ODEs
def model(y, t, Lambda_h, gamma, alpha, r, Lambda_m, beta,mu_m, p, q):
    S_h, I_h, S_p, R, S_m, I_m = y

    dS_hdt = Lambda_h + gamma * R - (alpha * I_m * S_h) / N
    dI_hdt = (alpha * I_m * S_h) / N - r * I_h + q*S_p
    dS_pdt = p*R - q*S_p
    dRdt = r * I_h - gamma * R - p*R
    dS_mdt = Lambda_m - (beta * I_h * S_m) / M
    dI_mdt = (beta * I_h * S_m) / M -mu_m*I_m

    return [dS_hdt, dI_hdt, dS_pdt,  dRdt, dS_mdt, dI_mdt]

# Objective function (sum of squared differences)
def objective(params, data, initial_conditions, t):
    Lambda_h, gamma, alpha, r, Lambda_m, beta, mu_m, p, q = params
    solution = odeint(model, initial_conditions, t, \
                      args=(Lambda_h, gamma, alpha, r, Lambda_m, beta, mu_m, p, q))
    model_infected = solution[:, 1]
    return np.sum((model_infected - data)**2)
```

Figure 4.1: Model and objective function codes

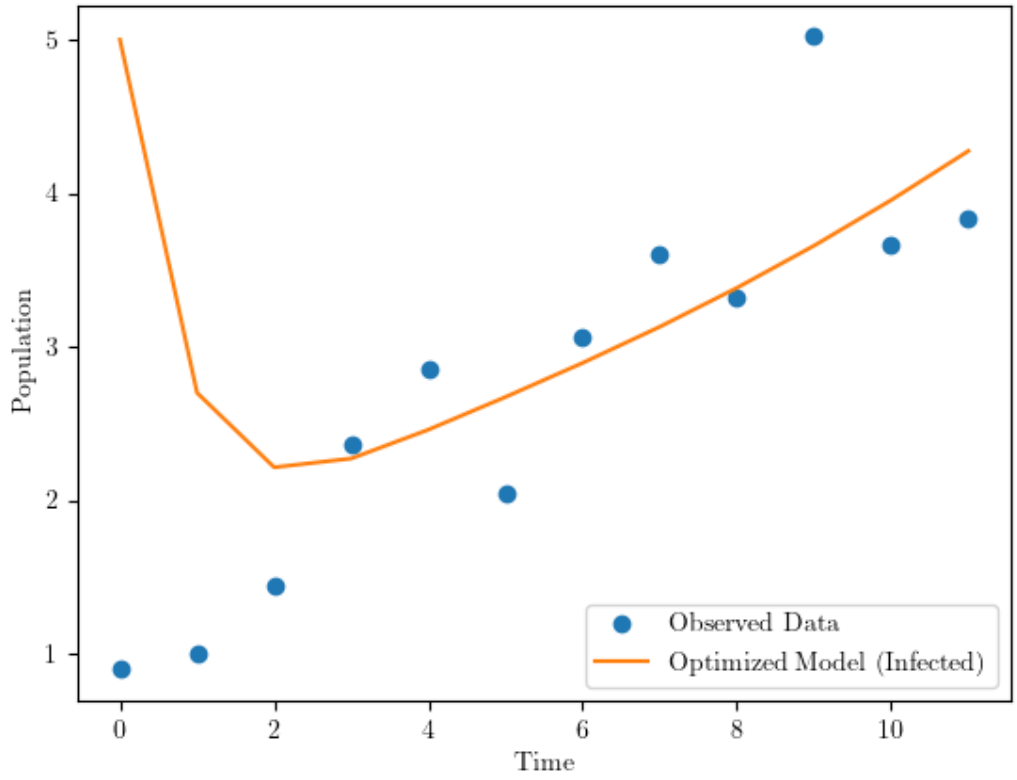

Figure 4.2: Comparison of the optimised model with the observed data

4.3 Simulation

The optimised parameters are substituted into the model equations as

$$\Lambda_h = 1, \gamma = 1, \alpha = 1, r = 0.39195362, \Lambda_m = 1, \beta = 1, \mu_m = 0.$$

To understand the response of each subpopulation to variation in the parameters, we say fix other parameters and vary one parameter.

4.3.1 Rate of human infection (α)

The susceptible human subpopulation gets infected when there is an interaction with an infected mosquito. The force of infection for the susceptible human subpopulation defined as

$$\frac{\alpha I_m S_h}{N},$$

is controlled by the value of α. Hence, variation in the rate of human infection is measured by the value of α. Figures (4.3) – (4.5) show the behaviour of the human subpopulations as the human infection rate increases. Figure (4.3) shows that the number of infected humans rises as the force of infection goes up. The heightened interaction rate leads to a corresponding increase in new

infections, amplifying the burden of malaria on the human population. This result aligns with the biological premise that greater exposure to infected vectors accelerates the spread of the disease. The increase in the infected subpopulation subsequently impacts other human compartments within the model. The increase in the number of malaria-infected humans also raises the number of humans who migrate to the recovered class. Figure (4.4) shows the increase in the recovered subpopulation as α grows larger. This rise reflects the natural progression of infections transitioning into recoveries through treatment or immunity. While recovery helps to reduce active infections, it also explains the heightened strain on healthcare systems as more individuals require medical attention and resources. Figure (4.5) shows a rise in the plasmodium-carrying human. As infected humans continue to rise, there will be an accumulation of treated humans free of the symptoms, but still carry the plasmodium and as a result can get sick once their immunity deteriorates a little. Individuals in this group, although free of active symptoms, retain the parasite and remain potential sources of infection if their immunity weakens. This trend highlights the latent risks associated with untreated or partially treated cases and the importance of sustained healthcare interventions. However, the susceptible human subpopulation decreases as α grows larger. This decline, illustrated in Figure 4.6, occurs as more individuals migrate to the infected class. Over time, the depletion of the susceptible population could influence transmission dynamics, potentially leading to reduced overall infections if combined with effective preventive measures such as vaccination, vector control, and public health education.

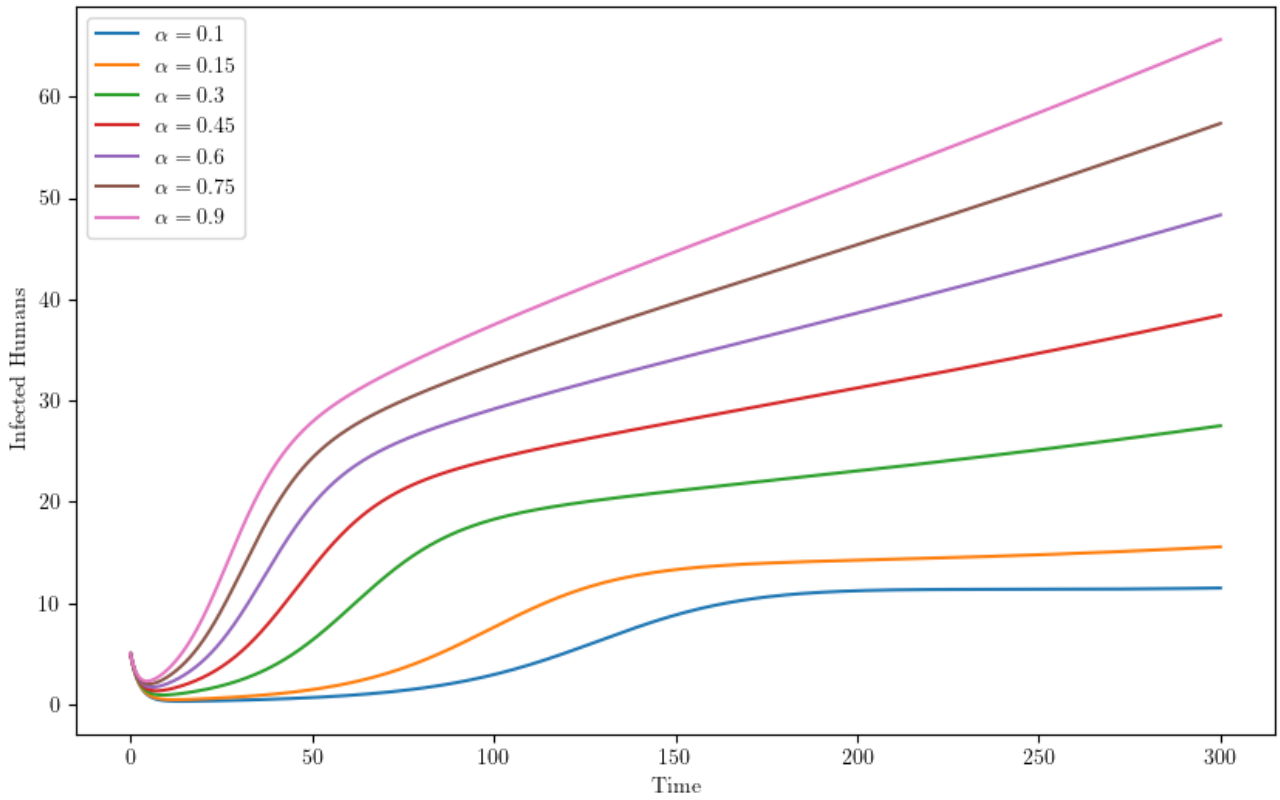

Figure 4.3: Infected Humans as α increases

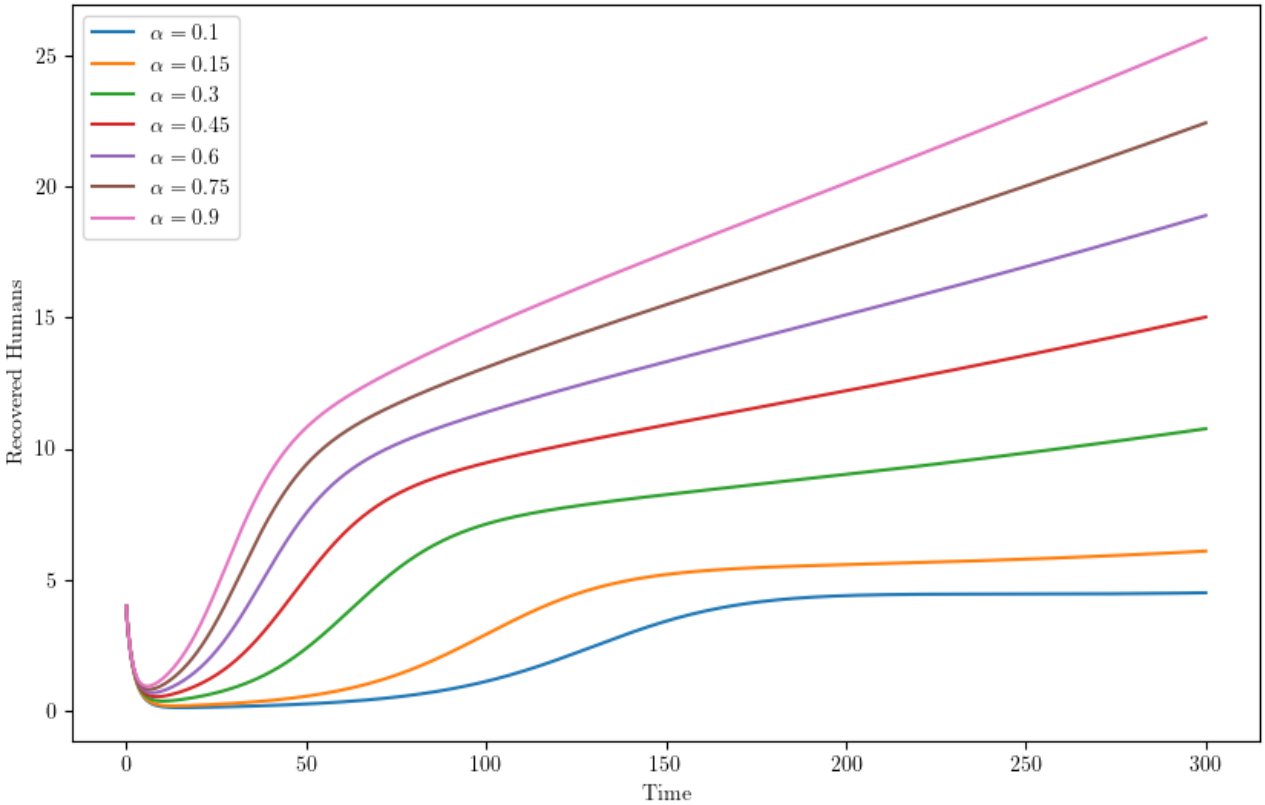

Figure 4.4: Recovered human as α increases

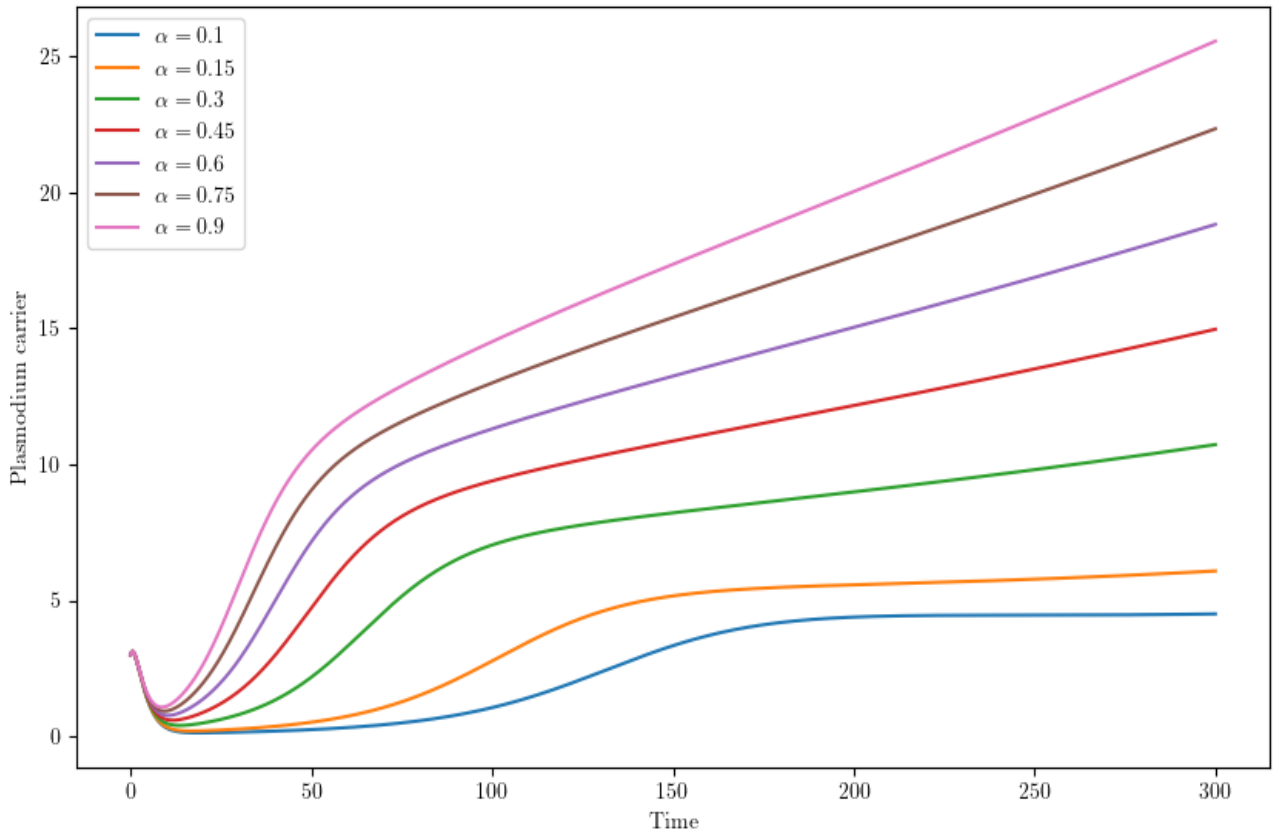

Figure 4.5: Plasmodium carrier as α increases

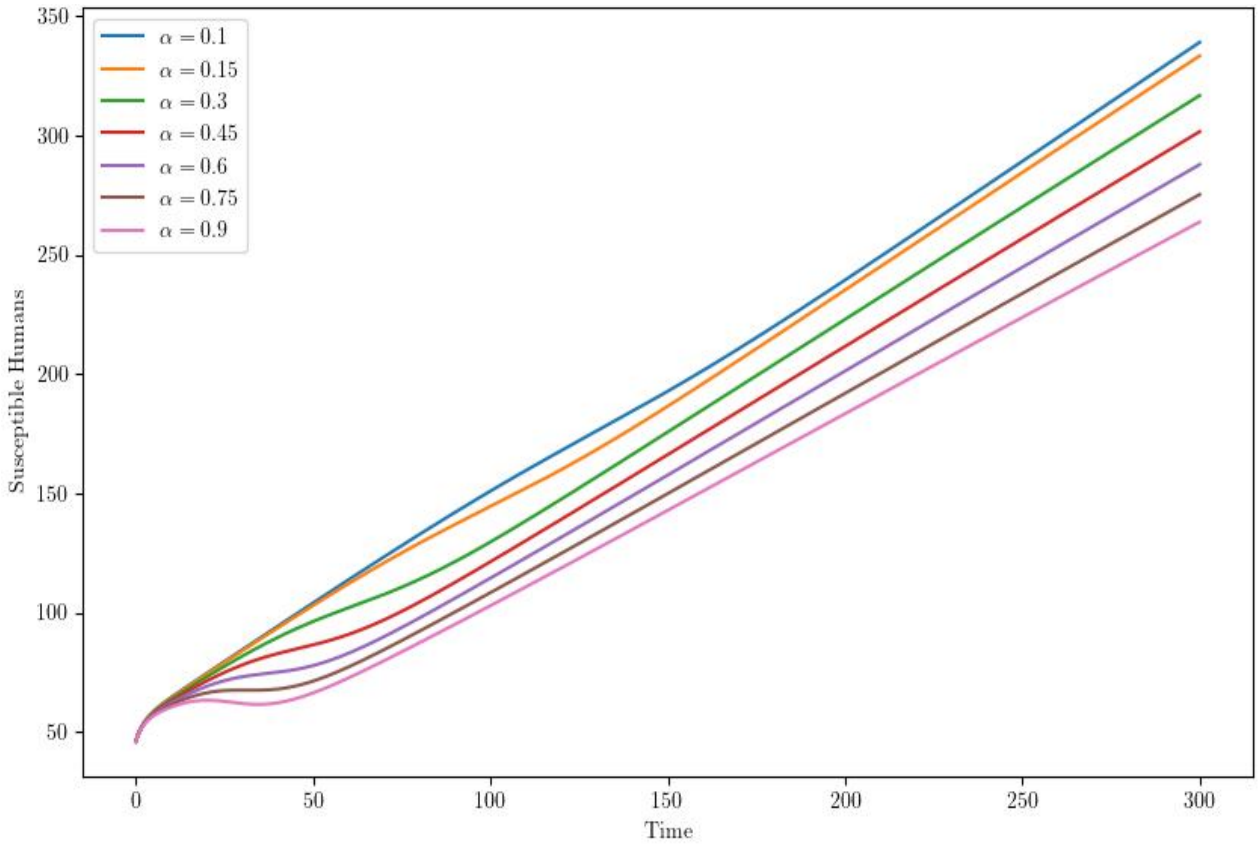

Figure 4.6: Susceptible human as α increases

4.3.2 Rate at which mosquitoes acquire the disease

Anopheles mosquitoes bite on a malaria-infected human to become infectious. The force at which the mosquitoes become infectious due to the interaction with malaria-infected human is defined as

$$\frac{\beta I_h S_m}{M},$$

and it is controlled by the value of β (the proportion of interaction that leading to infection). As the values of β is raised, the number of malaria-carrying mosquitoes is increased. This is well illustrated by the graph in figure (4.7). This increase reflects the enhanced transmission of the plasmodium parasite within the vector population, setting the stage for a higher force of infection on the human population. Increase in the number of mosquitoes that can infect human with malaria will definitely increase the number of humans who get bitten by the mosquitoes and as a result increase the number of humans who get infected with malaria. This is also illustrated by the graph of figure (4.8). The elevated transmission rate associated with an increase in β inevitably results in a decline in the susceptible human subpopulation. As more individuals are bitten and subsequently infected, the pool of uninfected humans diminishes. Figure 4.9 captures this decline, emphasizing the direct correlation between mosquito infection rates and the reduction in human susceptibility. The findings show the need for targeted vector control measures to manage the transmission dynamics influenced by β. Strategies such as the use of insecticide-treated bed nets, elimination of mosquito breeding sites, and application of indoor residual spraying are critical in reducing the mosquito population and lowering the value of β. These interventions not only decrease the infected mosquito population but also reduce the risk of human infections, thereby alleviating the overall burden of malaria.

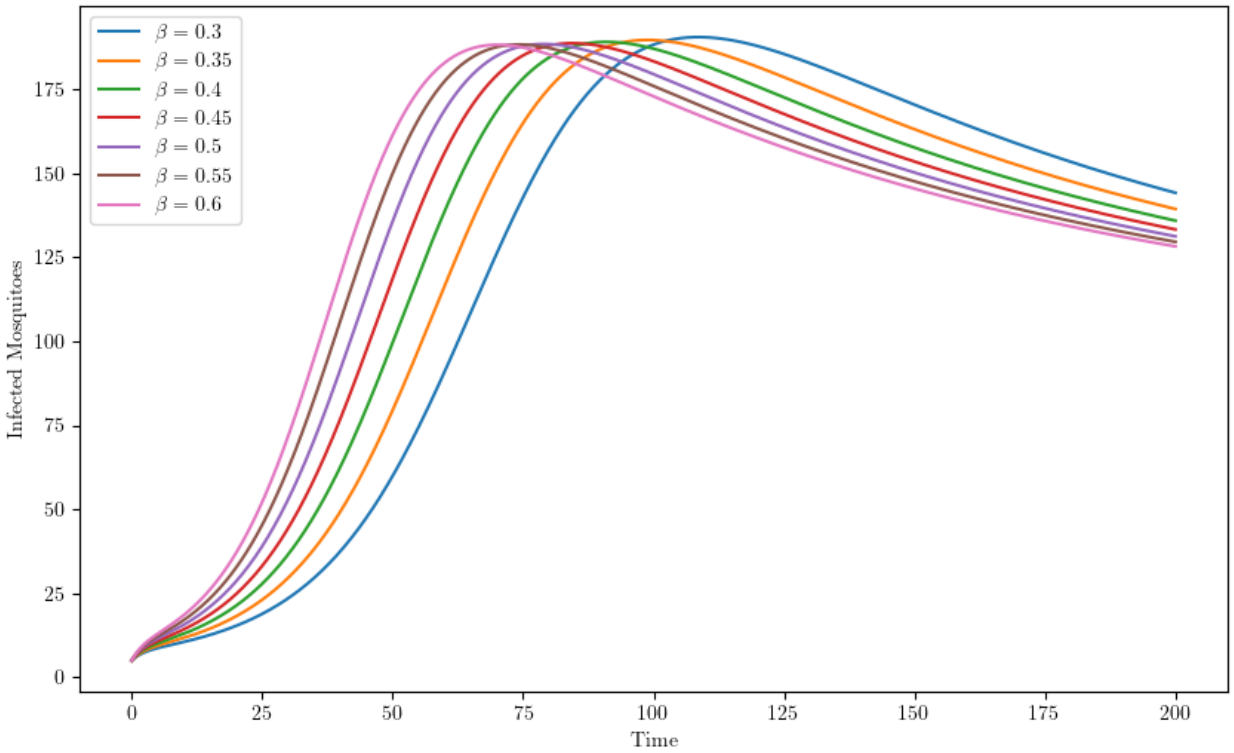

Figure 4.7: Infected mosquitoes with β

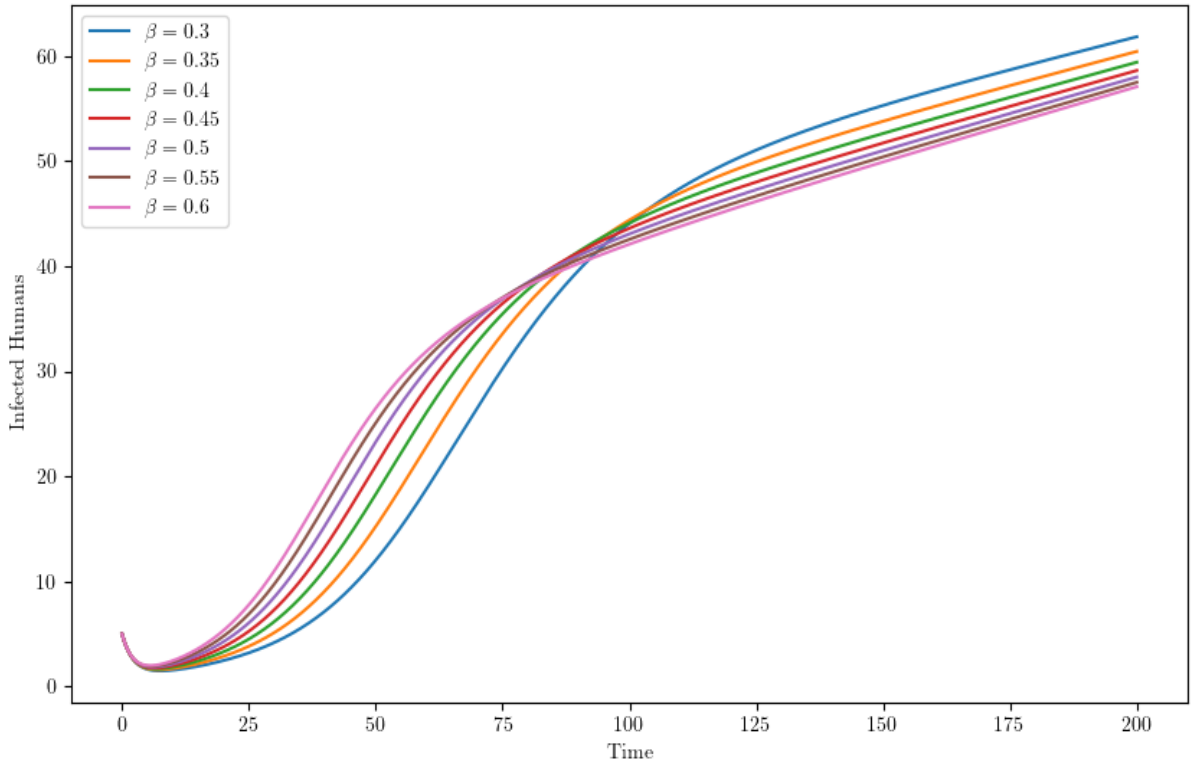

Figure 4.8: Infected human with β

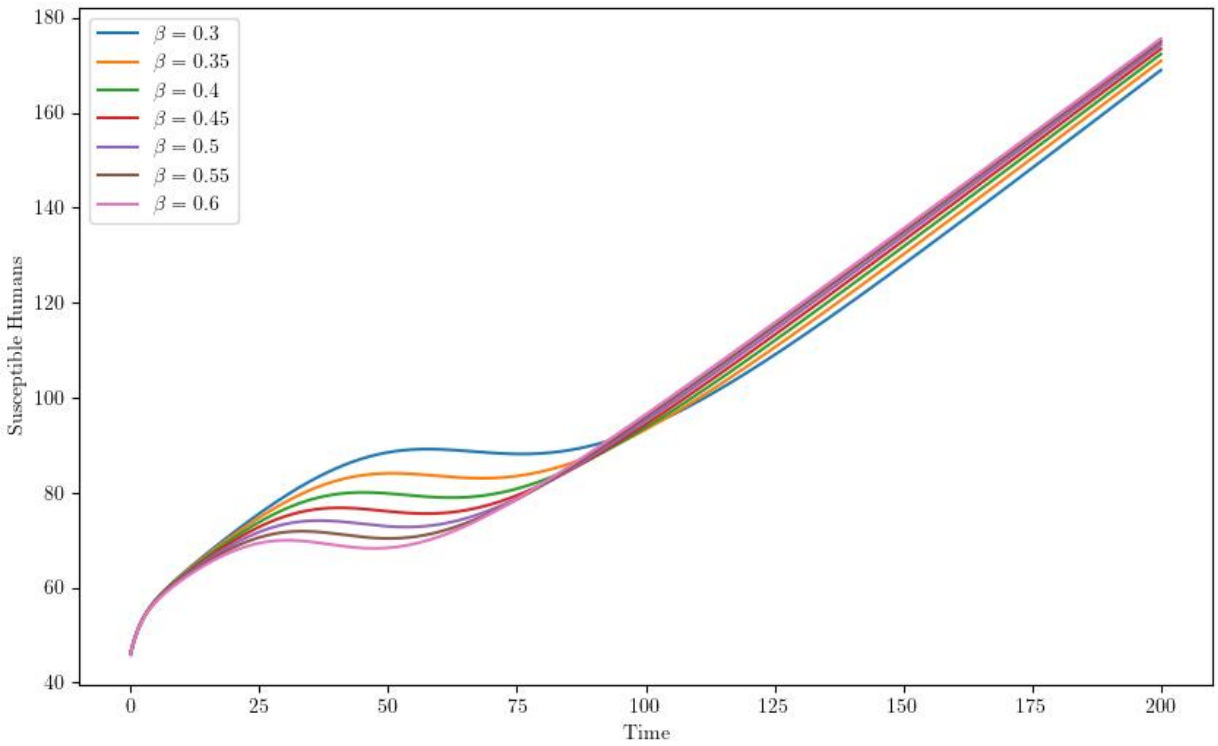

Figure 4.9: Susceptible human with β

4.3.3 Rate of Recovery

Humans recover from malaria either by the ability of their immune system to fight it off or by the administration of anti-malarial drugs. The rate at which any human recovers (by any approach) is denoted as r. By increasing the rate of recovery from malaria, the number of infected humans reduces. Evidenced by the graph in figure (4.10), as malaria-infected humans recover faster, the number of infected humans reduces significantly. It can be observed that the rate of recovery in the infected human subpopulation also reduces as r increases (check the distance between the consecutive graphs in figure (4.10). Due to the reduction in the infected human subpopulation, the exposure of mosquitoes to infected humans will reduce significantly and thereby ensuring that the infectious mosquito subpopulation reduces as r increases. This is typified in figure (4.11) where highest number of infectious mosquitoes occur at the lowest recovery rate r. Figure (4.12) shows the increase in the susceptible human subpopulation. This can be traced to the fact that a high percentage of recovered humans migrate to the susceptible class. Hence, an increase in the recovery rate r leads to migration of more humans into the

susceptible human subpopulation.

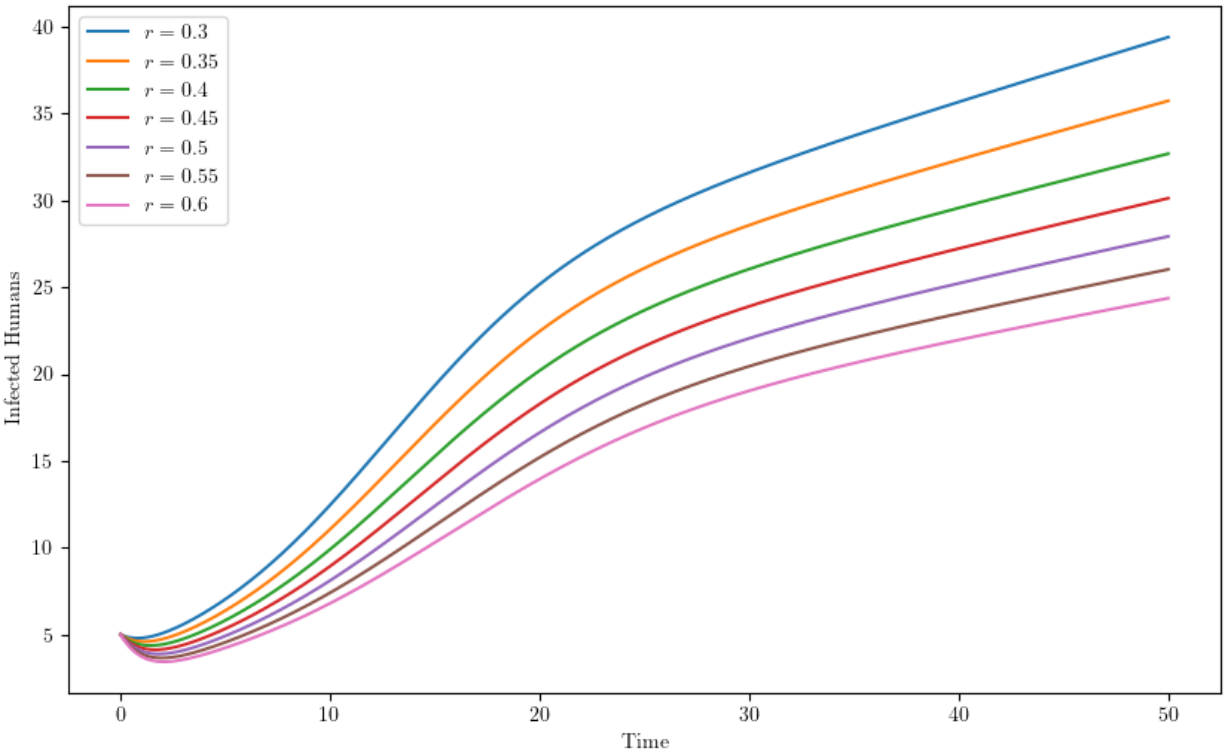

Figure 4.10: Infected humans with r.

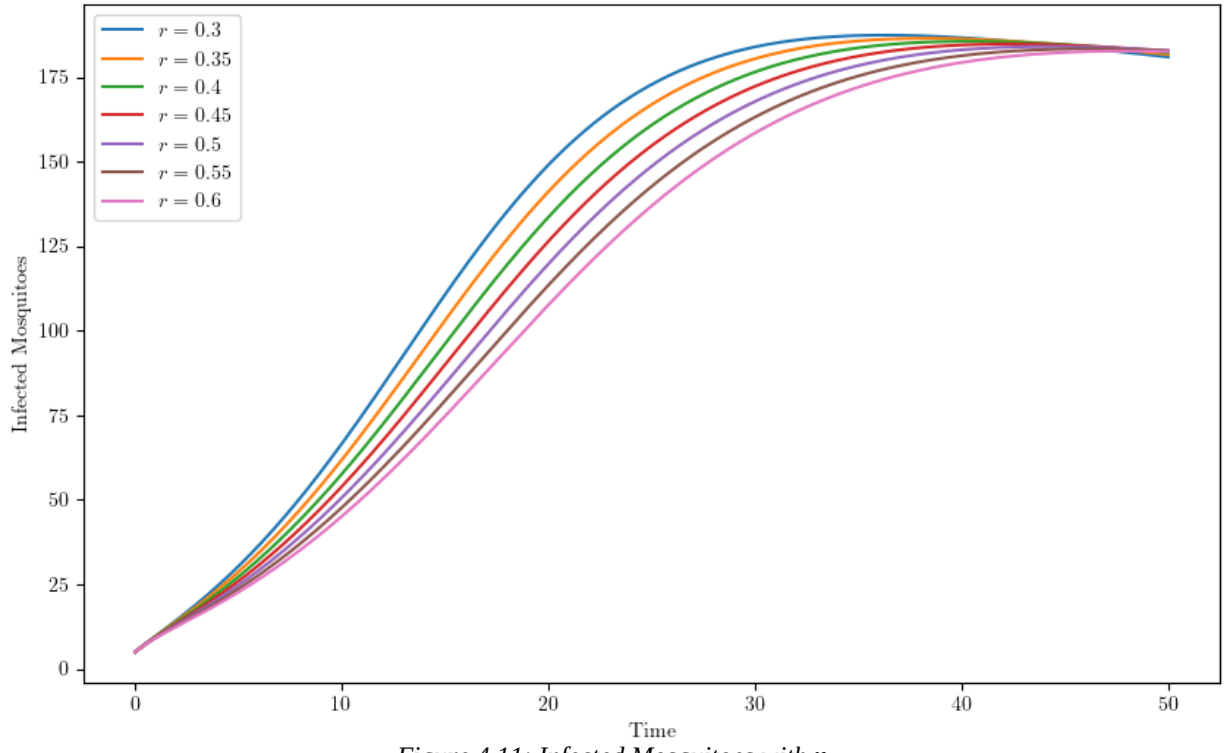

Figure 4.11: Infected Mosquitoes with r.

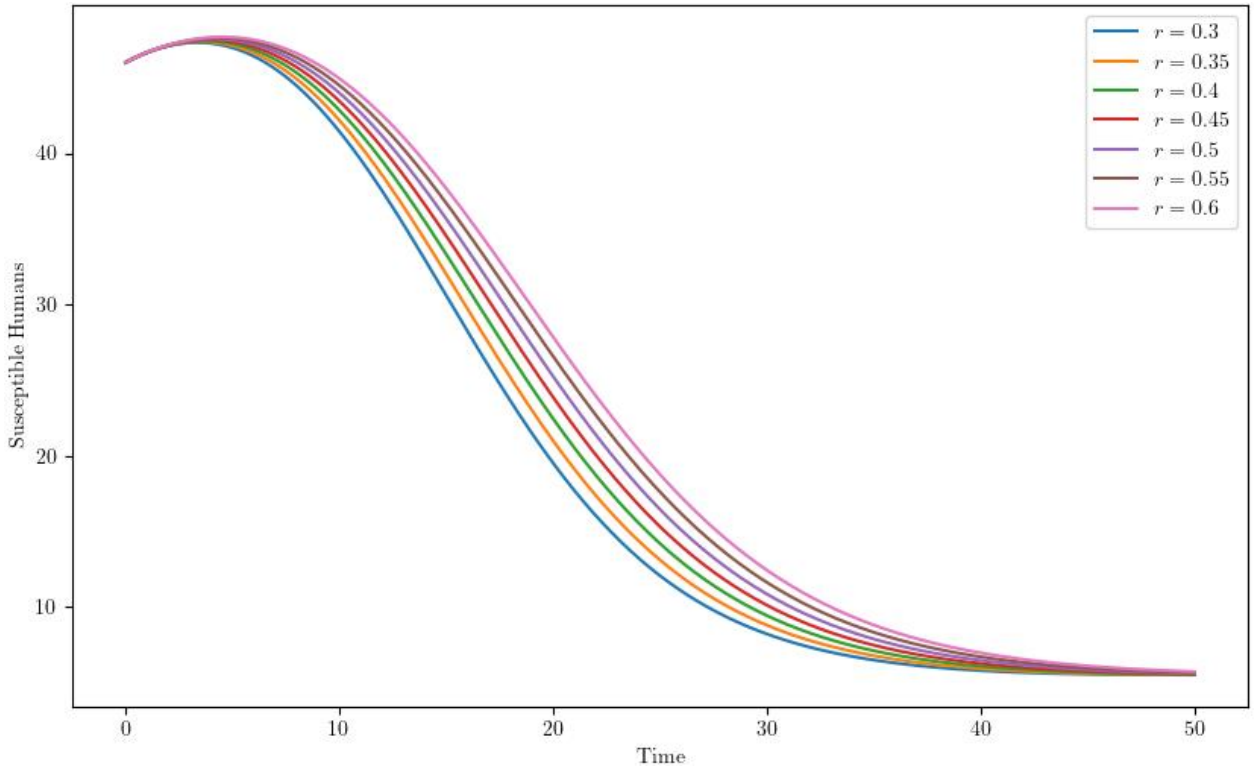

Figure 4.12: Susceptible humans with r.

CHAPTER 5

CONCLUSION AND RECOMMENDATION

5.1 Conclusion

This study has focused on malaria transmission between the human population in Busia County and mosquitoes in Busia County, Kenya, with emphasis on the optimisation of the model parameters. The study starts with a background information on the motivation behind this study, followed by a literature review that highlights existing studies. The model governing the transmission is developed as

$$\frac{dS_h}{dt} = \Lambda_h + \gamma R_h - \frac{\alpha I_m S_h}{N}$$

$$\frac{dI_h}{dt} = \frac{\alpha I_m S_h}{N} - rI_h$$

$$\frac{dR_h}{dt} = rI_h - \gamma R_h$$

$$\frac{dS_m}{dt} = \Lambda_m - \frac{\beta I_h S_m}{M}$$

$$\frac{dI_m}{dt} = \frac{\beta I_h S_m}{M} - \mu_m I_m$$

with the positive initial conditions

$$\begin{cases} S_h(0) = S_h^0 > 0, \\ I_h(0) = I_h^0 \geq 0, \\ R_h(0) = R_h^0 \geq 0, \\ S_m(0) = S_m^0 > 0, \\ I_m(0) = I_m^0 \geq 0. \end{cases}$$

Two reproduction numbers are expected in this case, since there are two interdependent populations. The reproduction number for the malaria infection in the human population is obtained as

$$R_{h,0} = \frac{\alpha}{r}$$

and the reproduction numbers for the mosquitoes to get infectious obtained as

$$R_{m,0} = \frac{\beta}{\mu_m}$$

The equilibrium points for the transmission of malaria between the human and mosquitoes' populations in Busia County, Kenya are obtained as the disease-free equilibrium

$$\left(S_h^{DFE}, I_h^{DFE}, S_p^{DFE}, {R_h}^{DFE}, S_m^{DFE}, I_m^{DFE}\right) = (\xi, 0,0,0, \sigma, 0)$$

where $\Lambda_m = \Lambda_h = 0$ and ξ, σ are arbitrary values.

The stability of the system is established and it is shown that the system is always stable when the subpopulations start in the neighbourhood of the disease-free equilibrium point. The numerical solution of the system is sought using an adaptive step-size Runge-Kutta-Fehlberg (RKF45) method. The parameter estimation was carried out by the using the Broyden-Fletcher-Goldfarb-Shanno (BFGS) method and the optimal parameter values are thus obtained as;

$$\Lambda_h = 1, \gamma = 1, \alpha = 1, r = 0.39195362, \Lambda_m = 1,$$

$$\beta = 1, \mu_m = 0, \qquad p = 0.72426444, \mathrm{q} = 0.23809668.$$

By studying the numerical solution, the following observations were made

i. the number of infected humans rises while the susceptible human subpopulation reduces as the force of infection goes up.

ii. As the values of β is raised, the number of infectious mosquitoes increases, the number infected humans increases and the susceptible human subpopulation drops.

iii. Increase in the rate of recovery from malaria reduces the number of infected humans, the infectious mosquito subpopulation reduces and the susceptible human subpopulation increases.

5.2 Recommendation

It is seen in this study that increase in the recovery rate of an infected human has the tendency to reduce infection in the human population. It is therefore recommended that anti-malarial drugs should be subsidised to allow more access to the medications. Secondly, further research should be carried out to estimate the potential significance of different anti-malarial medications. An

optimal pattern for the distribution of such drugs should also be obtained. Finally, availability of data is vital in optimising the parameter values. However, for this study, only data for 12 years (from year 2010 to 2021) was obtained and used for this research.

REFERENCES

Abimbade, S. F., Olaniyi, S., & Ajala, O. A. (2022). *Recurrent malaria dynamics: Insight from mathematical modelling.* The European Physical Journal Plus, 137(3),292.

Abongo, B. (2019). *Malaria vector surveillance in the context of enhanced vector control in western Kenya* (Doctoral dissertation, Liverpool School of Tropical Medicine).

Ahmed, N.; Macías-Díaz, J.E.; Raza, A.; Baleanu, D.; Rafiq, M.; Iqbal, Z.; Ahmad, M.O. (2022). *Design Analysis and Comparison of a Nonstandard Computational Method for the Solution of a General Stochastic Fractional Epidemic Model*. Axioms, 11, 10. https://doi.org/10.3390/axioms11010.

Aldila, D. (2022). *Dynamical analysis on a malaria model with relapse preventative treatment and saturated fumigation.* Computational and Mathematical Methods in Medicine.

Ale, S., Hunter, E., & Kelleher, J. D. (2024). Agent based modelling of blood borne viruses: a scoping review. *BMC Infectious Diseases*, *24*(1), 1411.

Amoo, O. M., Fagbenle, R. O., & Oyewola, M. O. (2022). *A Comparative analysis of numerical methods applied to nonsimilar boundary layer-derived infinite series equations.* Ain Shams Engineering Journal, 13(5),101713.

Andima, R. N., Mutuku, W. N., Farai, N., Awuor, K., & Oke, A. S. (2022). Mathematical Modelling of Diabetes under a Constrained Hospitalisation Resources. *Open Access Library Journal*, *9*(10), 1-14.

Bada, O. I., Oke, A. S., Mutuku, W. N., & Aye, P. O. (2021). Analysis of the dynamics of SI-SI-SEIR avian influenza A (H7N9) epidemic model with re-infection. *Earthline Journal of Mathematical Sciences*, *5*(1), 43-73.

Baihaqi, M.A.; Adi-Kusumo, F. (2020). *Modelling malaria transmission in a population with SEIRSp method*. In AIP Conference Proceedings; AIP Publishing LLC: Melville, NY, USA; Volume 2264, pp. 1–13. 6.

Bakary, T.; Boureima, S.; Sado, T. (2018). *A mathematical modelling of malaria transmission in a periodic environment.* J. Biol. Dyn., 12, 400–432.

Banerjee, P., & Sanyal, S. (2023). *Disease models in Malarial Research in Infectious Diseases Drug Delivery Systems*. Cham: Springer International Publishing, pp. 169-192.

Beretta, E.; Capasso, V.; Garao, D.G. (2018). *A mathematical model for malaria transmission with asymptomatic carriers and two age groups in the human population.* Math. Biosci., 300, 87–101.

Bashir, I. M., Nyakoe, N., & van der Sande, M. (2019). *Targeting remaining pockets of malaria transmission in Kenya to hasten progress towards national eliminating goals: an assessment of prevalence and risk factors in children from the Lake academic region.* Malaria journal,18,1-10.

Cai L, N. Tuncer, and M. Martcheva, (2017).” *How does a within-host dynamic affect population-level dynamics? Insights from an immune-epidemiological model of malaria*,”

Mathematical Methods in the Applied Sciences, vol. 40, no. 18, pp. 6424–6450.

Cai L.-M, Lashari A. A., I. H. Jung, K. O. Okosun, and Y. I. Seo, (2019).” *Mathematical analysis of a malaria model with partial immunity to reinfection”.* Abstract and Applied Analysis, vol., Article ID 405258.

Carrasco-Escobar, G., Fornace, K., & Benmarhnia, T. (2021). Mapping socioeconomic inequalities in malaria in Sub-Sahara African countries. *Scientific reports*, *11*(1), 15121.

Chen, S., Janies, D., Paul, R., & Thill, J. C. (2024). Leveraging advances in data-driven deep learning methods for hybrid epidemic modeling. *Epidemics*, *48*, 100782.

Djidjou-Demasse, R.; Abiodun, G.J.; Adeola, A.M.; Botai, J.O. (2020). *Development and analysis of a malaria transmission mathematical model with seasonal mosquito life-history traits*. Stud. Appl. Math., 144, 389–411.

DOMC, (2010). *National Guidelines for Diagnosis, Treatment and Prevention of Malaria in Kenya, Division of Malaria Control, Ministry of Public Health and Sanitation*, Nairobi, Kenya, 3rd edition.

Elnour, Z., Grethe, H., Siddig, K., & Munga, S. (2023). *Malaria control and elimination in Kenya: economy-wide benefits and regional disparities*. Malaria Journal, 22(1), 117.

Heath, K., Bonsall, M. B., Marie, J., & Bossin, H. C. (2022). Mathematical modelling of the mosquito Aedes polynesiensis in a heterogeneous environment. *Mathematical Biosciences*, *348*, 108811.

Ibrahim, M.M.; Kamran, M.A.; Naeem, Mannan, M.M.; Kim, S.; Jung, I.H. (2020). *Impact of Awareness to Control Malaria Disease: A Mathematical Modeling Approach.* Complexity, 1–13.

Kim, S.; Byun, J.H.; Park, A.; Jung, I.H (2020). *A mathematical model for assessing the effectiveness of controlling relapse in Plasmodium vivax malaria endemic in the Republic of Korea*. PLoS ONE, 15, e0227919.

Kimulu, A. M., Mutuku, W. N., Mwalili, S. M., Malonza, D., & Oke, A. S. (2022). Male circumcision: A means to reduce HIV transmission between truckers and female sex workers in Kenya. *Journal of Mathematical Analysis and Modeling*, *3*(1), 50-59.

Kimulu, A. M., Oke, A. S., Kimathi, M., Muli, C. N., Mwalili, S. M., & Mutuku, W. N. (2024). Mathematical model for impact of awareness on COVID-19 vaccination among the youth in Kenya.

Lashari, A. A., Aly, S., Hattaf, K., Zaman, G., Jung, I. H., & Li, X. Z. (2012). *Presentation of malaria epidemics using multiple optimal controls.* Journal of Applied mathematics.

Luo, D., Li, Y., Lu, J., & Yuan, G. (2022). *A conjugate gradient algorithm based on double parameter scaled Broyden-Fletcher-Goldfarb-Shanno update for optimization problems and image restoration.* Neural Computing and Applications, 34(1), 535-553

Mandal, S., Sarkar, R. R., & Sinha, S. (2011). *Mathematical models of malaria—A review*. Malar. J., 10, 1–19.

Mackinnon, M. J. (2005). *Drug resistance models for malaria*. *Acta*. Acta tropica, 94(3),207-217.

Mojeeb, A. L., Adu, I. K. (2017). *Simple mathematical model for malaria transmission*. J. Adv. Math. Comput. Sci., 25, 1–24. 17.

Montoya, C.; Romero-Leiton, J.P. (2020). *Analysis and optimal control of a malaria mathematical model under resistance and population movement.* arXiv, arXiv:2002.00070.

Montijano, J. I., Rández, L., & Calvo, M. (2024). *Explicit Runge–Kutta–Nyström methods for the numerical solution of second order linear inhomogeneous IVPs*. Journal of Computational and Applied Mathematics, 438, 115533.

Ogbaga, I. (2023). Artificial intelligence (AI)-based solution to malaria fatalities in Africa: An exploratory review.

Ogunmiloro, O.M. (2019). *Mathematical Modeling of the Coinfection Dynamics of Malaria-Toxoplasmosis in the Tropics*. Biom. Lett. 2019, 56, 139–163.

Oke, A. S. (2017). Convergence of differential transform method for ordinary differential equations. *Journal of Advances in Mathematics and Computer Science*, *24*(6), 1-17.

Osman, M., & Adu, I. (2017). *Simple mathematical model for malaria transmission*. Journal of Advances in Mathematics and Computer Science, 25(6), 1-24.

Olaniyi, S., Okosun, K. O., Adesanya, S. O., & Lebelo, R. S. (2020). *Modelling malaria dynamics with partial immunity and protected travellers: optimal control and cost-effectiveness analysis.* Journal of Biological Dynamics, 14(1), 90-115.

Pandey, R. (2020). *Mathematical Model for Malaria Transmission and Chemical Control withHuman-Related Activities.* Natl. Acad. Sci. Lett, 43, 59–65.

Rafia, G., He, J., Sana, D., Ebrahim, A. S. (2018). *A Simple SIR Mathematical Model of Malaria Transmission with the Efficacy of the Vaccine.* In Proceedings of the 2nd International Conference on Computational Biology and Bioinformatics, Bari, Italy, 26–28; 1145, 6–11.

Ross R. (1911). *Prevention of Malaria*, London, UK, 2nd edition.

Song, T.; Wang, C.; Tian, B. (2020) *Mathematical models for within-host competition of malaria parasites.* Math. Biosci. Eng, 16, 6623–6653.

Tchoumi, S. Y., Rwezaura, H., & Tchuenche, J. M. (2023). A mathematical model with numerical simulations for malaria transmission dynamics with differential susceptibility and partial immunity. *Healthcare Analytics*, *3*, 100165.

Traoré, B.; Koutou, O.; Sangaré, B. (2020). *A global mathematical model of malaria transmission dynamics with structured mosquito population and temperature variations.* Nonlinear Anal. Real World Appl, 53, 103081.

Traoré, B.; Sangaré, B.; Traoré, S. (2017). *A mathematical model of malaria transmission with structured vector population and seasonality.* J. Appl. Math, 1–15.

Wang, J., Zhao, H., & Wang, H. (2024). The role of natural recovery category in malaria

dynamics under saturated treatment. *Journal of Mathematical Biology*, *88*(3), 33.

WHO, World Malaria Report 2014, *World Health Organization, Global Malaria Programme*, Geneva,Switzerland, 2014, http://www.who.int/mediacentre/factsheets/fs094/en/

WHO (2021). *"World Malaria Report 2020". 20 years of global progress and challenges, 2020. World Health Organisation.* https://www.who.int/publications-detail-redirect/9789240015791789240015791-eng.pdf.

World Health Organization (2019). *World Malaria Report, World Health Organization*, Geneva, Switzerland.

Xue, C., Zhang, T., & Xiao, D. (2022). *An advanced Broyden–Fletcher–Goldfarb–Shanno algorithm for prediction and output-related fault monitoring in case of outliers.* Journal of Chemistry Advance online publication. https://doi.org/10.1155/2022/123456

Zafar, Z. U. A., Hussain, M. T., Inc, M., Baleanu, D., Almohsen, B., Oke, A. S., & Javeed, S. (2022). Fractional-order dynamics of human papillomavirus. *Results in Physics*, *34*, 105281.